

Oil and gas potential territories prediction based on remote sensing data. Case of: Skvortsivsko-Yuliyivsk test site of the Dnieper-Donets Depression of Ukraine

Rudarsko-geološko-naftni zbornik
(The Mining-Geology-Petroleum Engineering Bulletin)
UDC: 528.8; 553.9
DOI: 10.17794/rgn.2023.5.1

Original scientific paper



Artur Khodorovskiy¹; Alexander Apostolov²; Lesya Yelistratova³; Inna Romanciuc⁴

¹ State Institution "Scientific Centre for Aerospace Research of the Earth of the Institute of Geological Sciences of the National Academy of Sciences of Ukraine", Olesia Honchara Str., 55-b, Kyiv, 01054, Ukraine, ORCID: <https://orcid.org/0000-0003-2286-1517>

² State Institution "Scientific Centre for Aerospace Research of the Earth of the Institute of Geological Sciences of the National Academy of Sciences of Ukraine", Olesia Honchara Str., 55-b, Kyiv, 01054, Ukraine, ORCID: <https://orcid.org/0000-0003-3470-7613>

³ State Institution "Scientific Centre for Aerospace Research of the Earth of the Institute of Geological Sciences of the National Academy of Sciences of Ukraine", Olesia Honchara Str., 55-b, Kyiv, 01054, Ukraine, ORCID: <https://orcid.org/0000-0002-7823-5841>

⁴ LLC "UKLON UKRAINE", Stepan Bandera prospect, 20B, Kyiv, 04073, Ukraine, ORCID: <https://orcid.org/0000-0002-2891-4686>

Abstract

The methodological techniques developed were used to estimate the fracture permeability of rocks and predicting hydrocarbon reservoirs on the example of the Skvortsivsko-Yuliyivsk test site of the Dnieper-Donets Depression of Ukraine. The rock fracture permeability was estimated based on the interpretation of the lineaments field structural results by remote sensing data. The boundaries of 8 systems of lineaments and their modal values were selected, and the lineament density maps were compiled. The faults identified on the lineament density maps correspond to faults determined on the basis of geological and geophysical data. Maps of the summarized density of lineaments and their intersection nodes were compiled, which reflect the fracture permeability of rocks. Using spatial probabilistic forecasting techniques, it was found that all the maps of the lineament density field had an impact on the hydrocarbon reservoir placement (from 53% to 67.5% of the objects of study are allocated by separate systems) and were used to assess the territory potential for oil and gas exploration. The use of the complex function of the likelihood ratio made it possible to identify more than 90% of the study objects. Maps of the study area potential forecasting regarding the hydrocarbon reservoirs are compiled using the sliding window with size: 4.5 by 1.5 km and 14 by 4 km, which makes it possible to predict survey objects at different depths. 8 zones were selected based on the analysis of the complex probability function. There are 5 perspective areas selected, which make up 6% of the test site.

Keywords:

lineaments; remote sensing; oil and gas potential forecasting; perspective areas; Ukraine

1. Introduction

Studies using lineaments established on the basis of structural interpretation of remote sensing data have been developed in many researches. Hudson and Priest studied the rocks distribution and tried to relate the frequency of fractures in the image to the quality of rocks (Priest and Hudson, 1976; Hudson and Priest, (1979, 1983)). In the Koike et al., 1995 and Koike and Ichikawa, 2006 works, the linear features interpretation based on the remote sensing data were related to the tectonic features of the area. The researchers Lattman and Parizek, 1964 and Mabee et al., 1994 tried to link lineaments with groundwater resources. According to Kim et al., 2004, the occurrence of lineaments is closely related to groundwater searches. In this case, the identified number of lineaments in a defined area has a predictable

relationship with the flow rate of groundwater. Lineament studies were also based on magnetic field data (Henkel, (1979, 1992), Henkel et al., 2005, Oskooi, 2004). The lineaments identified by magnetic anomalies interpretation usually have a complex azimuthal distribution (Henkel, 1979). The automatic lineaments interpretation by computer programs is represented in works (Burdick and Speirer, 1980, and Raghavan et al., 1995). To analyse lineaments and construct lineament density maps, the researchers (Kim et al., 2004, and Mostafa and Qari, 1995) created a software product in the C language. There are three main approaches used by researchers in the processing of remote sensing data: manual (Leary et al., 1976, Ehman, 1985, Raj, 1989, Jordan and Schott, 2005), semi-automatic (Jordan et al., 2005, Juhari and Ibrahim, 1997, Lim et al., 2001) and automated (Jinfei and Howarth, 1990, Joshi, 1989, Kageyama and Nishida, 2000, Masoud and Koike, 2011, Mostafa and Bishta, 2005, Saadi et al., 2011).

Corresponding author: Alexander Apostolov
e-mail address: alex_aaa_2000@ukr.net

Researchers **Corte's, Arlegui, Soriano, and Casas** developed the LINDENS program for the lineament lengths and densities analysis. In addition, the authors specified the lineament conditions to belong to the averaging window and experimentally determined the limits of the square window averaging of lineaments for the construction of lineament density maps (**Arlegui and Soriano, 1998, Cortes et al., 1998, Casas et al., 2000**).

In structural geology, satellite images help to identify materials and their structure, regardless of their age and type of deformation (**Jutz and Chorowicz, 1993, Drury and Berhe, 1993, Nash et al., 1996**). The use of Digital Elevation Model (DEM), Landsat Enhanced Thematic Mapper Plus (ETM+) imagery, magnetic and gravity data for structural geology studies in special areas has enhanced interpretation and mapping capabilities (**Salehi et al., 2015**). (**De Oliveira Andrades Filho and De Fa'Tima Rossetti, 2011**) investigated the influence of lineaments on topography using SRTM (Shuttle Radar Topography Mission) and Advanced Land Observing Satellite Phased Array L-band Synthetic Aperture Radar (ALOS_PALSAR) data. **Magesh et al. (2012)** combined the methods of remote sensing data and geographic information system (GIS), which helped to reveal geological lines defining the regional distribution of groundwater. **Elmahdy and Mohamed (2016)** applied a Sobel filter to extract lineaments from Shuttle Radar Topographic Mission (SRTM) images and a DEM (Digital Elevation Model) studying the distribution of regular earthquakes in Egypt. **Eleni Kokinou and Costas Panagiotakis (2020)** carried out automatic recognition of tectonic lineament patterns in the morphology of the seabed to include the potentially hydrocarbon-rich areas in structural analysis. Percutaneous Coronary Intervention (PCI) Geomatics software was used to assess areas of geodynamic activity with the aim of automated selection of lineaments using DEM (**Zhantayev et al., 2017**). The other well-known works discussed the Landsat satellite images and DEM application for structural analysis and tectonic interpretation of the stable platform areas of Tunisia for identification of two main fault directions - 35°-65° and 110°-130° (**Chaabouni et al., 2012**). In the work (**Rawashdeh et al., 2006**), the authors proved that satellite monitoring is a useful tool for mapping the lithology of rocks using the remote sensing data to detect lineaments. In the work (**Sukumar and Nelson, 2017**), based on the image from the ASTER satellite, 4 different approaches to identify the lineaments were carried out in Ethiopia. The authors established that in terms of the optimal number of lineaments detected from the space image, the Li algorithm works better than other methods.

In the work (**Errami et al., 2022**) the method of principal component analysis (PCA) was used for Landsat 8 data for automatic lineament extraction in the south side of Marrakech High Atlas (Telouet-Tighza area). To observe the geothermal potential of northeastern Morocco

(**Redouane et al., 2022**) lineament analysis was used to identify the main faults and their directions. The determination of fault zones using the remote sensing data and GIS programs are given in (**Bishal et al, 2020, Azhar et al., 2022, Oluwaseun et al., 2022, Ahmadi and Pekkan, 2021**).

Gold mineralization in Eastern Cameroon was found to be spatially associated with lineaments/faults ranging from WNW-ESE to NW-SE (110-140). This shows a strong correlation with zones of medium and high density of lineaments (**Mbianya et al., 2021**). Researchers (**Mohamed, 2021**) used remote sensing and GIS data, namely, for the Landsat 8 satellite. The principal component analysis transformations produced saturated images and resulted in more interpretable images than the original data. X-ray fluorescence analyses prove that selected samples taken from the wall rock alteration zones are gold-bearing.

Additionally, researchers (**Nikulin, 2013**) used geoinformation technologies to solve forecasting and national resources search problems based on a complex of geological, geophysical and satellite data. In the tasks of finding and forecasting hydrocarbon reservoirs, lineaments were used by the following authors (**Pererva, 1999, Tovstyuk, et al., 2017, Patent, 2008; Lyalko, et al., 2010, Khodorovsky and Apostolov, 2012; Apostolov and Khodorovsky, 2017**).

2. Methods

As is known, the fracture permeability of rocks is determined by the number of fractures and their openness. In oil and gas provinces, where it is impossible to study crystalline rocks, lineaments obtained as a result of structural interpretation were used to identify cracks. Within each of the lineament systems, their openness was assumed to be constant. The value of lineament density is an estimate of the fracture permeability of rocks.

Evaluation of the rocks' fracture permeability based on remote sensing data, in accordance with the proposed methodology, includes the following steps:

1. Structural interpretation of remote sensing data and lineament map construction.
2. Analysis of the lineaments' orientation conformity and lineament systems selection (based on developed and implemented methodical approach).
 - 2.1 Quantitative description of the lineaments field using various indicators.
 - 2.2 Structural interpretation of lineament density maps of individual systems.
 - 2.3 Compilation of a fault map of the study area (based on lineament density maps of individual systems).
3. Estimation of the study area potential for the hydrocarbon reservoirs search based on lineament analysis data.

3.1 Analysis of the relationship between hydrocarbon reservoirs and lineament density fields of individual systems within the study area.

3.2 Maps of the probability ratio function values of the study territory analysis.

3.3 Placement patterns of perspective areas for hydrocarbon reservoirs search analysis within the study area.

3.4 Predictive assessment of the study area potential for the hydrocarbon accumulations search and the local perspective areas selection. Recommendations for further research.

2.1. Methodology of spatial probabilistic forecast

Spatial-probabilistic forecasting techniques make it possible to consider the nature of the objects' connection forecast with the individual features and to assess their cumulative impact on their placement. Additionally, at all forecast steps it is possible to perform the semantic control of the obtained results and promptly reject the errors.

The technique of spatial probabilistic forecasting is based on likelihood ratio functions for the entire range of values of the used features. The likelihood ratio function (F) is found as the ratio of probability density estimates of the two samples' feature value distributions - one-dimensional or multidimensional, that are characterized by a similar geological structure and the same degree of research areas. The first sample characterizes the feature value distributions located within the contours of forecast object points (OBJECT). The second sample is already an image of predictive object areas which are absent or their presence is unlikely (FON). Samples are formed by selecting values at evenly spaced points, so that $F = \text{OBJECT}/\text{FON}$.

First, graphs of the likelihood ratio functions are done for each feature used. Then the relationship between pairs of features is evaluated. For this purpose, two two-dimensional distributions are compared and a two-dimensional likelihood ratio function is compiled. In a similar way, the entire set of search features is considered. At the same time, it is not a simple summation of the informativeness of individual features, but the mutual connection and interdependence between features is taken into account. This leads to significantly increased informativeness and reliability of the forecast results. In addition, at all work steps, the content of intermediate results is monitored and, if necessary, all non-informative signs are rejected.

The value of the multidimensional function of the likelihood ratio, which takes into account the entire set of used features, is interpreted as an estimate of the probability of locating search objects at the points of the area with the corresponding features' values. The average density of forecast objects within the study area is taken as 1. The likelihood ratio function values, which exceeds 1, are characteristic of the forecast objects within the ar-

reas. The higher the value of the likelihood ratio function, the higher the density of forecast objects and the probability of their selection is observed. The obtained values of the likelihood ratio complex function are mapped by a system of isolines.

To assess the reliability of the compiled map, the likelihood ratio function values within the forecast objects were used for the complex function compilation, as well as those which were not involved for this purpose or for other reasons. In case of valid maps, all used objects, including training objects, will be characterized by elevated and maximum feature values.

Further analysis of the compiled map of the complex function values of the likelihood ratio for assessing the area prospects confirmed that, due to various reasons, the expert assessments of specialists and other available data were not taken into account. Based on the analysis, the forecast map of oil and gas capacity was compiled. The map shows prospective fields' spatial distribution patterns of various scales, including the local prospective areas. Besides, the recommendations were given on the sequence of carrying out further search works on them.

3. Results and Discussion

Following the proposed methods, the obtained results are presented according to the completed work steps.

3.1. Structural decoding of remote sensing data and lineament map creating

Considering the large size of the research area (total area 708.3 km², coordinate: upper left: X=35.51333°, Y=50.18899°, lower right: X=35.87675°, Y=49.94180°), the space images of the spring-autumn period with no clouds and haze from Landsat satellite were used to highlight the lineaments. Mostly synthesized images were interpreted, in cases where necessary integral (black and white) pictures were deciphered.

Structural interpretation of the images was carried out according to the contrast-analog decoding technique using various standard geoinicators. All lineaments were distinguished, regardless of their length, orientation, etc. The peculiarity of the interpretation was that the dimensions of each lineaments corresponded to the scale of the indicator to which it was established. Adjacent lineaments, regardless of the distance between them, did not merge into one lineament. During the interpretation process, considerable attention was paid to the rejection of anthropogenic origin linear forms of the image. These are the boundaries of forests, fields, various roads, strips of planted vegetation, arable land, dams, etc. In terms of remote observation of the basin, this is of particular importance, since the entire area of the depression has been subjected to significant anthropogenic influence over many years. In order to reject linear forms of anthropogenic origin, the interpretation results were compared

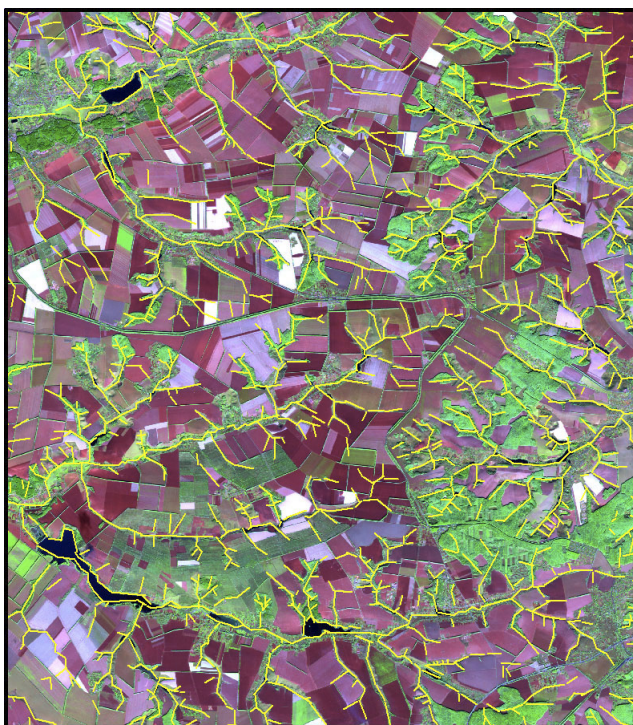


Figure 1: Map of the study area lineaments, based on the remote sensing data results interpretation, which is combined with a picture from the Sentinel-2 satellite, dated October 19th, 2018.

with various scales of topographic maps taken at different times.

Structural interpretation was carried out in the ArcGIS software for the test site and the adjacent area. The multi-zone space images from Landsat-8, Sentinel 1/2, topographic maps on a scale of 1:100,000, and a digital elevation model based on Shuttle satellite data were used. A total of 2140 lineaments were selected for study. The interpretation results are shown in **Figure 1**.

3.2. Analysis of the lineaments orientation regularity and lineament systems selection (based on developed and implemented methodical approach)

Many studies have established the regular nature of the spatial orientation of faults at all scale levels, from a separate slip to the entire planet. However, the number of fault systems and fracturing is distinguished by different researchers-from 2 to 34. As was observed by **Khodorovsky and Apostolov (2013, 2014)**, the reason is in the systems identifying methodology. The systems of faults and fracturing were established visually, based on the distribution graphs analysis of their extension azimuths. When compiling these graphs, different authors used an arbitrarily selected size of the measurement averaging window and, as a result, different authors analysed completely different graphs of the distribution of strike azimuths, which displayed structures of different scale levels.

Selection of lineament systems is important because all further processing of the lineament field is performed considering the limits of the established systems. Therefore, in order to get sufficiently objective data, we proposed certain requirements for obtaining graphs of the lineament extension azimuths and a probabilistic method of system selection.

According to the methodology proposed by **Khodorovsky and Apostolov (2013, 2014)**, the lineaments' orientation regularities analysis was carried out for the entire area using the statistical criterion Chi-square (X^2) to assess the reliability of the selection of maxima and minima on the histograms of the lineaments' orientation distribution. At the same time, our predecessors paid attention to the selection of individual maxima on the analysed distributions, which were considered as separate systems of lineaments. Analysis of the minima reliability has not been carried out by anyone, but its establishment is more important for further assessment of the lineaments density than the assessment of the maxima reliability. It is the minima that determines the lineament systems' boundaries, their width, and the lineament's number that will be assigned to a certain system.

Measurements of the lineaments' orientation were carried out within the separate areas, the number and size of which was determined by the need to obtain materials sufficient for further statistical processing. The reliability of the individual maxima and minima selection was assessed using the X-square test and received a score. Based on distribution analysis of the estimation point of the minima and maxima reliability selection, which was displayed in graphic form, 8 lineament systems were selected (see **Table 1**).

Table 1: Number, boundaries and modal values of lineament systems within the study area

System number	System description	System boundaries	Modal values of the system
1	West-Northwest	280°-300°	295°
2	Northwest	301°-320°	310°
3	Northwest	321°-340°	325°
4	Submeridional	341°-10°	355°
5	North-North-East	11°-35°	30°
6	North-East	36°-60°	50°
7	North-East	61°-75°	65°
8	Sublatitude	76°-279°	85°

The established lineament systems well correlate with the fault systems of Ukraine according to **Chebanenko, 1977, Tyapkin, 1998** and other Earth regions (**Moody and Hill, 1956, Shults, 1973, Halybina, 1975**). This indirectly testifies with the interpretation reliability, and to the fact that the established lineaments really correspond to the faults and native rocks fracturing.

3.2.1 Quantitative description of the lineaments field by various indicators

To assess the rock fracture permeability, the following quantitative indicators were used for lineament field characterization-the density of lineaments of individual

systems: the density of lineaments of all systems, and the density of nodes of lineaments intersection, which were measured within the sliding window. The determined indicator values were related to the center of the window. The research results were displayed in the form of isolines maps.

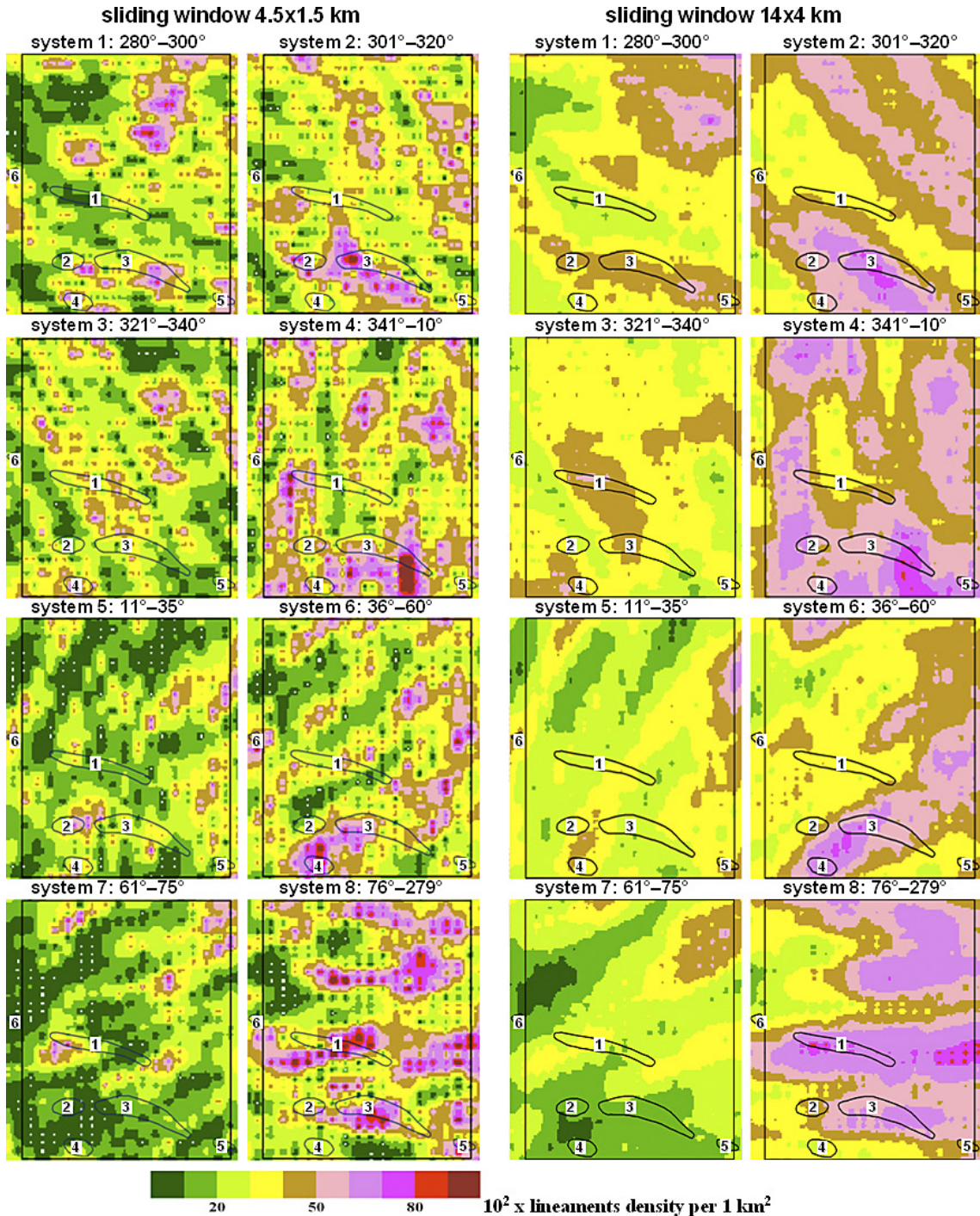



Figure 2: Density maps of individual systems lineaments compiled on the basis of the lineament map by Surfer software: system 1: 280°-300°, system 2: 301°-320°, system 3: 321°-340°, system 4: 341°-10°, system 5: 11°-35°, system 6: 36°-60°, system 7: 61°-75°, system 8: 76°-279°. The sliding window dimensions 4.5x1.5km and 14x4km.

Legend:

	Hydrocarbon reservoirs: 1 – West Skvortsivske, 2 – Mergynivske, 3 – Yuliivske, 4 – Naryzhnianske, 5 – Borchanivske, 6 – Kiyanivske
---	---

When compiling density lineament maps of individual systems, based on the linearly elongated shape of the lineaments, a window of the elongated shape was used for measurements. The long side of the window was oriented according to the modal value of each lineament system. A sliding window of isometric shape was used to compile the map of the lineaments density of all systems and the map of the intersection nodes of lineaments density. In this case, an elongated window will give preference to structures of a certain direction.

An important issue when compiling lineament density maps is the sliding window sizes choice. Two main factors influence the choice of sliding window sizes. First of all, the size of the window should ensure the presence of a sufficient number of lineaments in the majority of windows. In cases when in a significant number of windows (more than 10-15%) the values equal 0, the maps are difficult to interpret and they become uninformative. When using a window of considerable size in mapping, there is a probability of losing features of the density field of lineaments that are important for further research. In addition, when choosing the dimensions of the sliding window, the known dependence between the sliding window dimensions and the depth of hydrocarbon reservoirs should be considered. As evidenced by the data of exploration works within the study area the majority of gas and gas condensate deposits are located at more than 3100 m depths, while individual oil deposits are located mainly at shallower depths (Atlas, 1998). Therefore, 4.5×1.5 and 14×4 km size sliding windows were selected iteratively for the lineament density maps compilation, and two sets of lineament density maps were compiled accordingly. The size of the sliding window are chosen depending on the depth of oil and gas deposits. Size 4.5 by 1.5 km - characterizes oil and gas fields at a depth of approximately 3 km, a window of 14 km by 4 km - at depths of 5-7 km.

After determining the number of lineament systems, their boundaries, modal values, and sliding window sizes, lineament density maps of each of the eight systems were constructed. To do this, firstly, by applying the program developed by the authors, the values of lineament density indicators for different systems were calculated in a sliding window. The obtained results were presented in the format: Xcoord, Ycoord, Z, where Xcoord, Ycoord are the central coordinates of the sliding window in the rectangular coordinate system, Z is the value of the density indicators in the sliding window. The next step was focused on the lineament density maps compilation in the Surfer software in *.grd format and conversion to the Erdas Imagine program using the Import / GRD (Surfer:ASCII/Binary) procedure. Next, these maps were colored according to the lineaments density value (see Figures 2 and 3).

On the lineament density maps of individual systems, up to 10 fields with different density values have been distinguished (see Figures 2 and 3). On all compiled

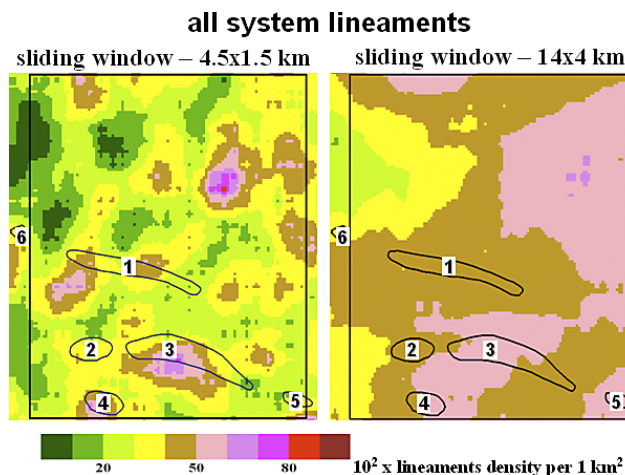


Figure 3: Density maps of all lineaments, compiled on the basis of the lineament map by Surfer software. The sliding window dimensions 4.5×1.5km and 14×4km.

maps, the density fields of systems 2 (Northwest), 4 (Submeridional), 6 (Northeast) and 8 (Sublatitude) are marked by the highest values of lineament density. On the lineaments density maps of systems 2, 4, 6 and 8, the fields of increased density values by the size of area they occupy significantly outweigh the fields with minimum and low values. On the density maps of systems 1, 3, 5, and 7, on the contrary, the field areas with low density values prevail in size over the field with increased density values.

On the separate systems lineaments maps, prevailing in the size of the density field, correspondingly high or low values are marked by a clearly elongated shape. That is why they differ from the shape of fields with intermediate values of density, which are close to an isometric shape. Fields with different density values on lineament density maps of all systems have a shape close to the latter.

3.2.2 Structural interpretation of individual systems lineament density maps

For interpretation of the lineament density maps of various systems, their comparison with the structural maps of previous research works was carried out (Havrysh, 1969, Baghriy, 2013). It is proven that the large, long faults established according to the data of geological and geophysical studies are located in the fields with the maximum and increased values on the lineament density maps of the corresponding systems. Thus, on the lineament density map of the second system (North-west), the field of increased values of lineament density corresponds to that part of the Northern Marginal Fault (Havrysh, 1969), which is located within the polygon. Similarly, the density maps of the fourth (sub-meridian), sixth (North-eastern) and eighth (sublatitudinal) lineaments systems are somewhat smaller in size than the Northern Fault. Large regional faults and individual faults composing them coincide with the local absolute or relative maxima of the lineaments density. This was the basis for the faults selection within the

study area based on the lineament density maps and the compilation of the fault map data.

As a result of the lineament density maps' interpretation, more faults were established than were identified by predecessors based on geological and geophysical data. As evidenced by special studies at the Kursk aerospace testing ground, to distinguish the matching number of faults in accordance with remote and geological-geophysical surveys, the latter should have an order of magnitude more detail. In contrast to the traditional fault selection in line form, on lineament density maps, the faults are displayed in the form of different width, length and intensity zones, which reflects changes in the structure of faults along their extension.

Analysis of the total density lineament maps. Total density lineament maps, compiled using windows of different sizes, are generally similar to each other, but also have differences. On both maps, the fields of high and maximum values of the total density of lineaments are located mainly in the south, near the Northern Marginal Fault of the Dnieper-Donets Depression, and in the Northeast of the area, where, according to the predecessors data (Havrysh, 1969), there is a large-scale fault that runs parallel to the Northern Marginal Fault of the Dnieper-Donets Depression. At the same time, on the map made up of a smaller window, it can be seen that the field of high and maximum values is located mainly in the South-East of the area and is limited by the field of lineaments density low values of the North-Eastern extension. It is possible that these discrepancies reflect the structure peculiarities of the district at different depths.

Analysis of the lineament intersection nodes map. According to many researchers, intersection nodes of faults in different directions are important for the hydrocarbon reservoirs placement. It is evident that the nodes will be characterized by an increased number of fractures in different directions and significant spatial heterogeneity of the structure. These are metastable states of rock zones characterized by high instability of the rock destruction processes. Such structures have a shape close to isometric and will be characterized by increased permeability of rocks, both the foundation and the sedimentary cover. Practically, the nodes of faults intersection observations are carried out very rarely, especially in oil and gas-bearing areas, that is connected with the difficulties of performing such surveys.

Based on the structural interpretation data of the images and developed methodical approach, a map of the nodes of lineament intersection density was compiled (see Figure 4). The map was developed using a 3×3 km sliding window, where dimensions are chosen experimentally. To facilitate the further description, the places of maximum and increased values on the map of the lineament intersection node density, received the following numerical designations (9.1 – 9.5). Observing the map of lineament intersection nodes, they are unevenly located on the study area and prevail in the southeastern

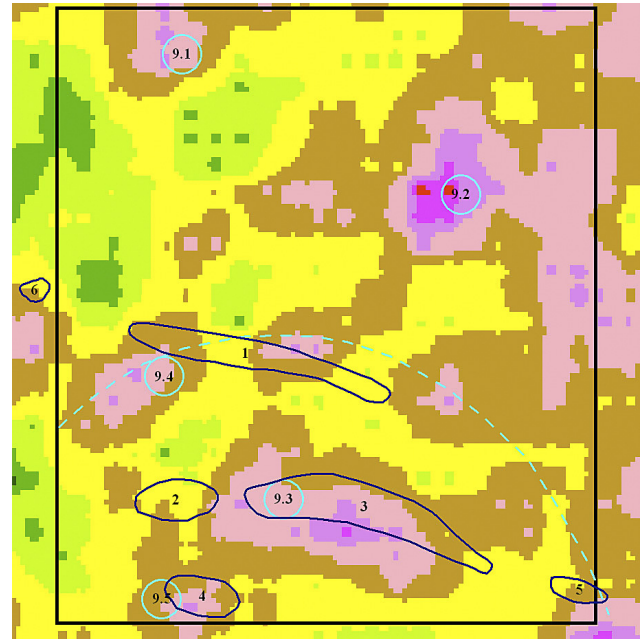


Figure 4: Lineament intersection node density map with highlighted anomalous values

part. The most intensive anomaly of the intersection node density is located in the Northeast of the square. This does not contradict the visual comparison with the previous structural studies (Baghriy, 2013).

Analysis of the relative distribution of individual anomalies in the node density over the area reflects that they are placed regularly. Thus, relatively large in size and intensity anomaly 9.3, within which the Yuliyivske deposit is located concentrically, at a distance of up to 10 km, is smaller in area and intensity anomalies, two of which coincide with the well-known Skvortsivske and Narizhnianske deposits. A similar distribution of small anomalies of the lineament intersection node density relative to larger anomalies is observed in relation to anomalies 9.1 and 9.2, but it is less clearly expressed. The same regularity has the ring structures distribution, which were often observed by remote sensing data, but still their geological nature has not been investigated. It is possible that the isometric nature of the anomaly distribution of lineament intersection nodes is related to the presence of degassing pipes (Kropotkin, 1985), but this requires further investigation.

3.2.3 Fault map of the study area (according to lineament density maps of individual systems)

Using the established connection of the fields of increased lineament density values of all systems with known faults, the fault selection was carried out in accordance to the lineament density maps of individual systems and a map of polygon faults was compiled (see Figure 5).

The largest in length and manifestation intensity in the lineament density fields are the following stretches -

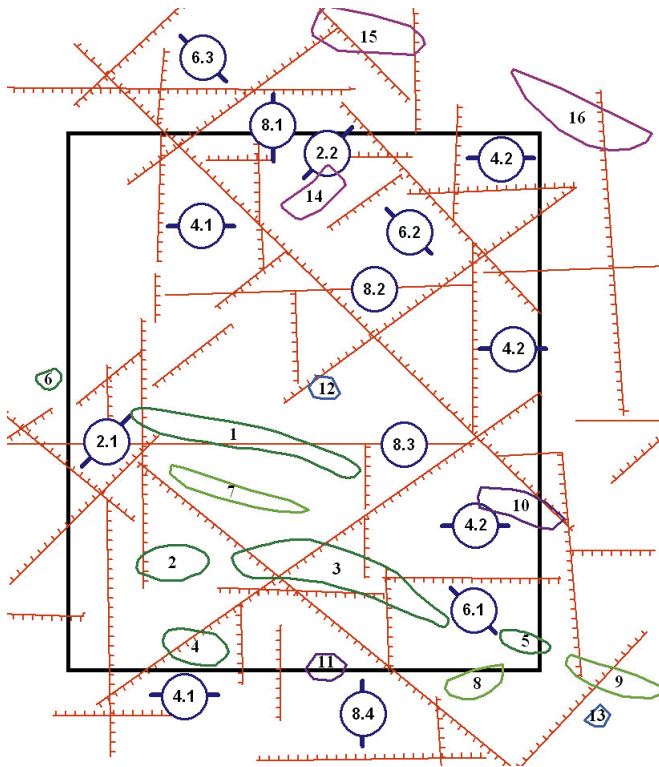


Figure 5: Map of polygon faults, compiled based on the analysis of lineament density maps of individual systems

Legend:

	Edge faults of fault zones		Fault zone numbers
	<p>Hydrocarbon reservoirs: 1 – West Skvortsivske, 2 – Merchynivske, 3 – Yuliivske, 4 – Naryzhnianske, 5 – Borchanivske, 6 – Kiyanivske, 7 – Povdenoskvortsivske, 8 – Ohultsivske, 9 – Karavanivske.</p> <p>Objects included in the drilling fund: 10 – Hukivske, 11 – Hryntsivske.</p> <p>Prospective oil and gas facilities (NGPO): prepared for deep drilling: 12 – Nedilne, 13 – East Karavanivske, detected by seismic survey: 14 – Taverivska, 15 – Filativske, 16 – Baklanivske.</p>		

Northwest (system 2), Meridional (system 4), Northeast (system 6), and Latitudinal (system 8). On the lineament density maps of systems 1, 3, 5, and 7, the fields of increased lineament density are insignificant in length, and the corresponding faults are probably of secondary importance. Discontinuous faults of various azimuthal systems detected within the North Side will differ among themselves, according to the nature of geodynamic and morphokinematic characteristics.

The fault map shows the most significant faults, which had the greatest impact on the test site structure. In order to facilitate the description of selected faults, they received a numerical designation, where the first

digit corresponds to the number of the fault belonging to the system, and the second - the fault serial number within the system.

The fault map (see **Figure 5**) shows two Northwest-striking fault zones 2.1 and 2.2. Fault zone 2.1 is located within the Northern Marginal fault zone, which separates the Northern side of the Dnieper-Donets Depression from the graben and plays an important role in the emplacement of explosive deposits within the Dnieper-Donets Depression. All known accumulations of both hydrocarbon reservoirs and structures, which were shown on the structural map along the reflective horizon Vb2 coincide with the zone extension (**Structural and tectonic map, 1996**). As evidenced by the lineament density map of system 2, the averaging window is 14×4 km, this zone is quite narrow, has a relatively simple structure and is characterized by a sufficiently high intensity of lineament density. Within the polygon boundaries, it consists of two fairly long faults, which are placed in a stage-like manner, not as a single linear structure. On the system 2 map, an averaging window of 4.5×1.5 km, which characterizes the lower depth located structures, this zone consists of two less clearly defined faults. Modern geological and geophysical studies have proven that the Northern Marginal Fault is not a single linear structure - a slide with 1-2.5 km amplitude (**Baghriy, 2013, Baghriy et al., 2007**). Within the study area and in the adjacent territory, the Northern marginal fault is represented by a zone of sub-parallel discharges of relatively small amplitude. A significant number of perspective horst anticline zones were discovered here. Like other Northwestern faults, the Northern edge of the fault zone is direct strike or strike-slip (**Baghriy, 2013, Baghriy et al., 2007**).

To the northeast of the Marginal fault zone, about 20 km distance, there is another zone of increased density values of northwest-trending lineaments, which is designated as fault zone 2.2. The existence of such faults zone was reflected by **Havrysh (1969)** on the basis of geophysical survey data. In the density field of lineaments, these two fault zones differ from each other in the nature of the structure and intensity of reflection. Zone 2.1 is characterized by a relatively simple structure and a small width within the test site. When folding it, the faults are placed in a stage-like manner. While zone 2.2 has a much larger width, its structure clearly shows two bounding edge faults that are parallel to each other. More than ten local structures of various types have been identified within its boundaries (**Structural and tectonic map, 1996**). However, the territory of the zone has not been sufficiently studied, only 6 wells have been drilled within the zone, which are mainly located outside the boundaries of these structures. Of these wells, one produced oil, one produced gas, and the last produced water. A significant number of perspective areas within the zone have also been established according to the structural and atmogeochemical studies data (**Baghriy, 2013**).

All of the above suggests that fault zone 2.2 has a certain influence on the hydrocarbon reservoir placement and requires further research.

According to the density maps of meridional lineaments (system 4), two fault zones 4.1 and 4.2, with the distance between 15-18 km, are established within the polygon. Both fault zones were confidently reflected on the density maps of lineaments compiled by both a large and a small window. They are characterized by fairly high density values. Within them, separate faults are located linearly, in contrast to system 2 faults.

Within the range, both fault zones are divided into northern and southern parts by a single strip of low density values of Northwest-trending lineaments. The southern and northern parts of faults 4.1 and 4.2 are located, respectively, within fault zones 2.1 and 2.2. Moreover, the boundary between the northern and southern parts of faults 4.1 and 4.2 coincides with the boundary between fault zones 2.1 and 2.2. This fact confirms the leading role of Northwest-trending faults in the test site structure.

The selected fault zones coincide with the fault zones that were established earlier and where temperature increases are recorded in individual areas (Baghriy, 2013). It is possible that both of these zones are connected with the Orekhovo-Kharkiv deep fault located outside the polygon (Havrysh, 1969). Fault zones 4.1 and 4.2 are deep structures with a long history of evolution. On the southern extension of these structures, in the places of their intersection with the Northern side border, a sharp change in the extension of the border of the side is recorded (Structural and tectonic map, 1996). This was pointed out by many researchers and associated with the change of strike with the movement of blocks along meridional faults (Chirvinskaya and Sollogub, 1980, Garetsky et al., 1988).

According to the lineament density map, the structures of the northeastern extension (system 6) are generally characterized by high density values, and local fields of increased density values in most cases have a significant length. The analysis of the density maps proved that there are three fault zones on the studied area. Fault zone 6.1, located in the southeast of the test site, is the largest in terms of length and intensity of manifestation. Zone 6.2 in the center of the polygon is significantly inferior to the previous fault zone in terms of the intensity of the lineaments density and the length of individual local structures. Within these fault zones, the local faults composing them are characterized by a considerable length and a mostly linear mutual arrangement. Outside the polygon, this structure coincides with the zone of the horizontal gradient high values of the field of gravity anomalies (Baghriy, 2013).

Fault zone 6.3, located in the Northwest of the test site, is a small fragment of a large fault zone located outside the study area.

Probably, system 6 faults are part of the Odesa deep fault zone, which is a component of the transregional

zone of deep faults crossing the entire territory of Ukraine (Garetsky et al., 1988). The deep penetration of these faults into the earth's crust is also indicated by the presence of radon anomalies within them (Baghriy, 2013, Baghriy et al., 2007). Movements in the zone were shear or shear-rotational in nature. (Chebanenko, 1977, Chekunov and Pashkevich, 1989). This is an ancient deep structure, which was reflected in the structure of the lithosphere. It developed particularly actively and continuously from the Mesozoic to the modern tectonic activation (Garetsky et al., 1988). Perhaps this is due to its relatively insignificant role in the process of hydrocarbon reservoirs formation.

Sublatitude faults related to system 8 are widespread throughout the territory of the test site and the adjacent area. All of them appeared with approximately the same intensity on the corresponding density maps of lineaments compiled using a larger and smaller sliding window. According to lineament density maps, sublatitudinal faults are characterized by a significant length and linear arrangement of the faults that make them up. Directly within the boundaries of the test site, there are 4 fault zones, with a distance 8-10 km, which can be traced far beyond the boundaries of the study area. According to regional studies, the entire territory of the test site is located within the regional Sublatitude fault zone, which runs through the entire territory of Ukraine and continues beyond the state borders (Atlas, 2001). The length of this zone only within the borders of Ukraine is more than 1100 km with an average width of 30 km. Within the boundaries of the Ukrainian Crystalline Massif, where this zone is well studied, it coincides with the well-known Kyiv-Hadyach and Andrushov-Khorol-Rososhan faults, which had an influence on the structure of the Ukrainian Crystalline Massif since the late Proterozoic (Havrysh et al., 1989).

Thus, the conducted study proved that all faults known according to the data of geological and geophysical surveys correspond to anomalous values of the density fields of the corresponding systems. According to the lineaments density maps, there are more faults than were established according to the geological and geophysical data. Faults selected by the lineaments density maps do not contradict the geological and geophysical research data.

3.3 *The potential of the test site territory estimation for the hydrocarbon reservoirs searches based on lineament analysis data*

It is known that the fracture permeability of rocks is simultaneously affected by cracks of different orientations and nodes of their intersection, but their influence on rock permeability is different. Therefore, for a predictive assessment of the territory prospects, it is necessary to evaluate the cumulative effect on the rock permeability of cracks of different orientation, which is not equal

to the usual sum of the effects of individual crack systems, but has a much more complex nature of dependence. The cumulative effect of the above-mentioned structures on the localization of hydrocarbon reservoirs and the predictive assessment of the prospects of the territory for their search was observed on the basis of spatial-probabilistic forecasting method (Nagorsky et al., 1971, Patent, 2010).

3.3.1 Analysis of the relationship between hydrocarbon reservoirs and lineament density fields of individual systems within the test site

During the test site research, as primary information about hydrocarbon reservoirs, information about their location within the study area and the boundaries of the deposits according to the structural-tectonic map along the Vb_2^n reflective horizon was used (Structural and tectonic map, 1996).

A visual analysis of the specified hydrocarbon reservoir location within the lineament density fields of both all systems and individual systems proved that they are simultaneously found in fields with different lineament densities. Hydrocarbon reservoirs are rarely found in fields with high, especially maximum, and minimum lineament density values. They are mostly located in fields with intermediate values of lineament density. Such a complex nature of the hydrocarbon reservoir connection with the lineament density fields of various systems does not allow for the visual and objective solving of the deposit forecasting problem. The higher the likelihood ratio function value, the closer the relationship between the lineament density values and the search objects and vice versa. Accordingly, perspective areas are characterized by function values greater than 1.0, and the larger the function value, the higher the potential of the area for hydrocarbon reservoirs search.

The values of the function in the interval from 0 to 1 correspond to those values of the lineaments density that have no connection with the search objects. Areas characterized by function values less than 1.0 are unperspective for the hydrocarbon reservoirs search. Establishing such areas is an important task because it reduces the size of the territories where it is expedient to conduct search and reconnaissance work.

Values of the function that are equal to 1.0 indicate that the distribution of the trait within the boundaries of deposits and beyond them does not differ. The corresponding sign is not informative for finding hydrocarbon reservoirs. Areas characterized by such values of the function refer to those whose prospects cannot be determined based on lineament analysis. Other methods should be used to assess their prospects.

The results of the evaluation of the likelihood ratio function values for different values of the density fields of lineaments on the corresponding maps of all systems are compiled using a sliding window of 4.5×1.5 km size.

The obtained data analysis proved:

- 1) all the analyzed signs are related to the search objects and therefore all of them are search signs and should be used for the hydrocarbon reservoirs prediction;
- 2) the vast majority of search objects are located in fields with intermediate values of lineament density and nodes of their intersection, the boundaries of these intermediate fields are established; which are different in different signs;
- 3) high values of the lineament density within the search objects are rare, they occupy from 0 to 3% of the area, and only for the lineament density maps of systems 3 and 6 are 9 and 5.5%, respectively;
- 4) within the study objects, low values of the lineament density of systems 1, 2, 6 and 7 do not occur at all; of systems 3, 4, 5 and 8 occupy 12-27% of the area, nodes of intersection of lineaments and the sum of lineaments of all systems occupy about 10% of the area;
- 5) for all lineament density systems, the relationship with the objects of study was calculated using the likelihood ratio function, which, respectively, is: system 1 – 53%, system 2 – 67.5%, system 3 – 54%, system 4 – 65%, system 5 – 59%, system 6 – 55%, system 7 – 67%, and system 8 – 60%.

After establishing the relationship of hydrocarbon reservoirs with all individual features, according to the spatial probabilistic forecasting technique, individual features were integrated and the total likelihood ratio function was calculated. This function made it possible to establish the influence of the sum of the used search features on the hydrocarbon reservoirs placement. Using the composite function, the values of the probability function were calculated for each point of the study area in accordance with the values of search features that characterize each point of the polygon. In order to visualize the obtained results and their analysis, a map of the likelihood ratio function values in the isolines was compiled.

3.3.2 Analysis of maps of the probability ratio function values of the test site territory.

The assessment of the study area potential based on the complex of search features established according to lineament analysis data was carried out using the spatial-probabilistic forecasting technique. According to the nature of the hydrocarbon reservoir distribution by depth within the test site (Atlas, 1998), two maps of the complex function values of the likelihood ratio of the area were compiled using a sliding window of 4.5×1.5 and 14×4 km. Based on the previous researchers' studies and our experience, maps made using a smaller window characterize the prospects of placing deposits up to a depth of 2.5-3 km, while maps made with a larger window characterize the prospects of the area up to a depth of about 7 km.

On both maps, the values of the complex functions of the likelihood ratio vary from 0 to > 5.0 . The obtained function values show how many times the probability of detecting hydrocarbon reservoirs in each point of the area is higher or lower than that which would be obtained in the case of drilling the territory according to a uniform grid, without taking into account search features. For the analysis and further use of the compiled maps for solving search and reconnaissance tasks, the obtained values of the likelihood ratio functions on the maps compiled by windows of different sizes were combined into five populations that differ in perspective.

The first set of data is characterized by complex function values from 0 to 0.9. Areas that correspond to these values are unperspective for prospecting. Such areas cover the largest territory on both maps. For the effectiveness of the search for hydrocarbon reservoirs, the establishment of such areas is very important, because it allows you to significantly reduce the area of research and concentrate efforts on perspective areas. As a result, funds and time for conducting research will be saved.

The second set of data is characterized by complex function values from 0.9 to 1.01. Areas with these function values refer to those within which the proposed research method is not informative. On both maps of the complex probability functions, they cover insignificant areas and therefore they were not separated, but were combined with the first set.

The third set of data is characterized by the values of complex probability functions from 1.01 to 1.5. Areas characterized by such values of the likelihood ratio functions are classified as prospective areas.

The fourth set of data with values of complex probability functions from 1.5 to 2.0 which are characterized by increased perspective.

The fifth set of data is characterized by the highest values of the complex probability functions greater than 2.0 and characterize areas with high prospects.

A comparison of the areas sizes covered by the aggregates of the complex probability function values showed that they successively decrease from those occupied by the lowest values of the functions (the first + second sets) covering the largest area to the smallest areas occupied by the highest values of the function. This should be expected if the function values really characterize the territory prospects.

According to the data of the one-dimensional probability function, perspective areas occupy from 53% to 67.5% of the territory of the research objects, and according to the data of the complex probability function - more than 90%.

After compiling the maps of complex probability functions, the reliability of the compiled maps was assessed by establishing to what extent they are confirmed by the available geological material - the results of exploration and exploitation works, previous geological and geophysical studies and other data. For this purpose,

the distribution of the complex probability function values was analyzed within the boundaries of the known deposits on the study area - Skvortsivske, Merchykivske, Yuliyivske, Narizhnianske, and the Ogultsivsk deposit located on the test site. The distribution of the function values within the Kiyaniv deposit, located near the western border of the test site, was analyzed. The analysis shows that the majority of all deposits in the area, especially the most productive, on both composite maps of complex probability functions, are characterized by high and maximum values of probability functions. Moreover, the most productive fields, Skvortsivske, Yuliyivske, Narizhnianske, are characterized by the highest probability function values (4 and 5 set of data). And this despite the fact that the productivity of deposits was not taken into account during the study. The established fact makes it possible to rank the research area according to the degree of productivity.

The Karavanivske and Ogultsivske deposits, which are small in size and are located outside the test site and whose data were not taken into account in the forecasting process, are also characterized by the probability function values, which are perspective. However, they are characterized by lower function values, which does not contradict the data of reconnaissance works within them (Atlas, 1998).

Thus, the results of the reliability analysis of the likelihood ratio functions values maps allow to state that the compiled maps really reflect the features of the hydrocarbon reservoirs distribution within the test area. They can be used to analyze their placement regularities within the studied area and to predict the prospective assessment of the area for the new hydrocarbon reservoir search.

3.3.3 Analysis of perspective areas placement patterns for the hydrocarbon reservoir search within the test site

A comparative analysis of the maps of the likelihood function complex values placement, compiled using different sized windows (see Figure 6) proved that, in general, they are similar to each other in many respects.

On both maps, prospective areas are highlighted, and they are made up of two scale level objects. Those larger in size were identified as perspective areas, and smaller in size, located within them, as perspective structural zones. In the process of analyzing the regularities of the perspective areas spatial distribution within the test site, the fault map of the study area was taken into account, as compiled from the lineament density maps of individual systems.

Both analyzed maps show that perspective areas are located throughout the test site, but the density of their location on the area and the value of the potential within their limits change naturally. Within the test site, two

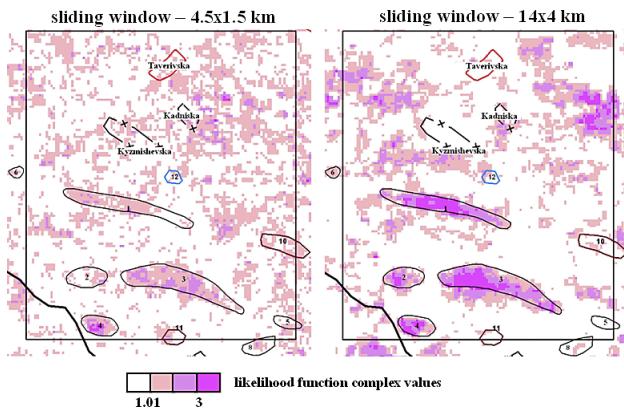


Figure 6: Maps of the placement of the likelihood function complex values, compiled using a sliding window of the size: 4.5x1.5 km and 14x4 km.

perspective areas were selected - the southwestern and northeastern, which differ both in terms of the size of individual perspective areas and in the values of perspective, which were estimated by the complex function values. The boundaries of these two areas on the analyzed maps generally coincide.

Both prospective areas are stretched along large Northwest-striking faults 2.1 and 2.2. The border between these two areas is generally defined by the Southern Marginal Fault of fault zone 2.2. The border is better visible on the complex likelihood ratio function map, which is made up of a smaller window.

The southwestern prospective area is located along Fault 2.1, which belongs to the Northern Marginal Fault of the Dnieper-Donets Depression. This is a large deep fault with a long evolution history, which is assigned the main role in the formation of both the general structural plan of the Northern side of the Dnieper-Donets Depression and the local structures complicating it. The northern marginal fault, like other northwestern faults, is characterized as a direct strike or strike-slip that dips in the western direction. According to all researchers, the Dnieper-Donets Depression and the Northern Marginal Fault have little significant influence on the hydrocarbon reservoir formation in the region.

Based on these studies, the southwestern prospective area mainly coincides with the Southern mobile structural-tectonic zone of the starboard side (Baghriy, 2013, Yevdoshchuk et al., 2001) and with the Yulia-Markiv oil and gas bearing zone of the subregion of the North side (Yevdoshchuk et al., 2001).

The northeastern prospective area, like the southwestern area, is closely related to the Northwest-striking fault zone 2.2. According to available geophysical data, this zone is smaller in depth of structure penetration than fault zone 2.1. On the lineament density map of system 2, on which this zone is established, this zone is characterized by slightly lower values of lineament density. However, this fault zone has not been sufficiently studied and requires further research.

According to our data, this perspective area coincides with the zone of low-amplitude structures or the Turutynsko-Chabanivsko-Romanivsk oil-and-gas-bearing zone of low-amplitude structures (Baghriy, 2013, Yevdoshchuk et al., 2001).

According to the complex probability function maps, the southwestern region is much more perspective than the northeastern one. The last occupies a small area within the test site, and for a more thorough assessment of its prospects, research should be conducted on a larger area.

Within both perspective areas, separate perspective zones with a linear shape are distinguished. The orientation of the selected perspective zones coincides with the fault zones, which are established according to the lineament density maps of various systems and shown on the composite fault map (see Figure 7). The distribution of hydrocarbon reservoirs and oil & gas prospective objects outside the test site, both on the territory of the North Side and the adjacent part of the graben, where they make up separate zones (strips) with different orientation in space, has a similar nature of distribution. This indicates that these zones are controlled by faults of different orientations.

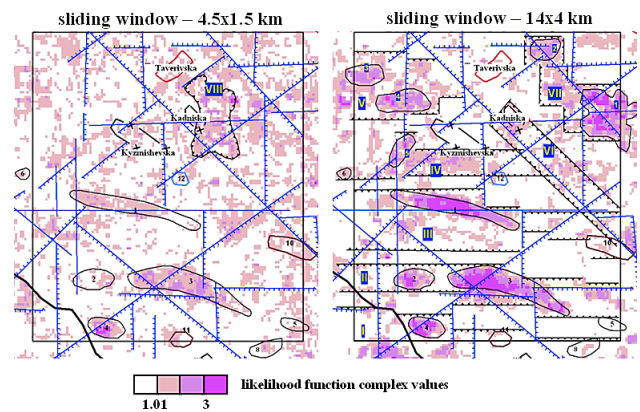


Figure 7: Forecast maps of the test site territory potential for the hydrocarbon reservoir search, compiled using a sliding window of the size: 4.5x1.5 km and 14x4 km.

Legend:

	Forecast zones		Forecast zone numbers
	Local perspective areas		Numbers of local perspective areas

A total of 7 zones (strips) are distinguished within the test site based on the complex probability function map analysis, which were numbered from 1 to 7 for ease of description. These zones are characterized by an increased density of perspective values and higher values than in the areas that limit them. In the south-western region, 5 perspective areas of mainly sub-latitude, sometimes north-western direction are visually highlighted.

Prospective zone 1 (*Narizhnyanska*) is located along the southern border of the test site and beyond. The extent of the zone is Sublatitudinal. The zone was better reflected on the complex probability function map values, compiled using a window of smaller size (4.5×1.5 km). Within the zone boundaries the Narizhnyansk deposit and the Hrynkiivsk structure are located, as well as the Ogultsivsk, Karavanivsk and Marinsk deposits, which are located outside the test site, but at a slight distance. The zone is located within the large Sublatitudinal fault zone 8.4.

Prospective zone 2 (*Yuliyivska*) is located along the northern border of Sublatitudinal fault zone 8.4, but outside the zone. The zone was better reflected on the complex probability function map values, compiled using a window of 14×4 km. The Naryzhnian and Yuliyiv deposits are located within the zone.

Prospective zone 3 (*Skvortsivska*) is located along a latitudinal fault. The zone was better displayed on the values of the complex likelihood function map, which is made up of a larger window. The Skvortsiv deposit is located within the zone. It is possible that the Pivdenoskvortsivska and Gukivska structures belong to the zone.

The first three perspective zones described above were highlighted by our predecessors (**Baghriy, 2013**). This testifies of the obtained forecast results reliability, and the next two perspective zones were not previously identified.

Prospective zone 4 (*Nedilna*) is located between two latitudinal faults 8.2 and 8.3 and is characterized by the smallest area and low values of prospectivity. The zone was clearly visible on the values of the complex probability function map, which was compiled using a window of 14×4 km. On a similar map, made with a smaller window, the zone was practically not revealed. Nedilna, Kuzmychivska and other structures are located on the periphery of the zone, but their prospects have not been assessed. In the west, the zones are extended, but the small Kiyanivske deposit is located outside the test site (**Structural and tectonic map, 1996**).

Prospective zone 5 is located between fault zones 8.1 and 8.2, which are crossed by Submeridional fault zone 4.1. The zone appears only on the map of the complex likelihood function, compiled using a 14×4 km window, and is not displayed on the map compiled with a smaller size window. The territory of this zone, like zone 4, has not been sufficiently explored and needs further study.

A characteristic feature of the structure of these five zones is the clearly identified influence of Submeridional faults on the distribution of perspective values in the plane. In many cases, Submeridional faults limit fields with different values of perspective.

Two perspective zones 6 and 7 were established within the northeastern prospect area, which were better shown on the complex probability function map, compiled using a 14×4 km window. These zones differ from

the prospective zones of the southwestern region in terms of their spatial orientation. They are stretched in the Northwest direction according to the marginal faults of fault zone 2.2. as well as mostly lower values of the assessment of the territory's prospects.

Prospective zone 6, unlike other zones, is characterized by the lowest density of prospective fields within the zone, as well as the lowest values of prospectivity. The zone is selected only on the complex probability function map, compiled using a window of 14×4 km.

Prospective zone 7, in contrast to the previous zone, is characterized by a larger size of area, as well as higher values of perspective. In terms of its prospective values, it can be compared with the first three zones of the southwestern region, where hydrocarbon reservoirs are known.

Perspective zone 8 stands out well only on a perspective map made using a smaller window (see **Figure 7a**). In terms of prospective values, it is slightly inferior to the prospective zones of the southwestern region of the test site. The well-known Kadnytsk and Taverivsk structures are located on the border of the zone. Part of its territory is located within the prospective areas established according to the atmogeochemical data.

3.3.4 Predictive evaluation of the test site potential for the hydrocarbon accumulation search and the selection of local perspective areas. Recommendations for further research

According to the complex values of the likelihood ratio function maps, compiled using sliding windows of 4.5×1.5 km and 14×4 km sizes (see **Figure 6**) the research area is undoubtedly perspective for further searching of hydrocarbon reservoirs. This is evidenced by the fields with sufficiently high perspective values, the location of which relative to the area faults are similar to the location of known hydrocarbon reservoirs.

When selecting local perspective areas, the values of perspective, the area sizes, their location relative to the selected faults, and the previous studies data were considered. First of all, these are drilling and atmogeochemical surveys data.

Local-perspective areas were identified within 4, 5 and 7 structural-tectonic zones, where only part of their territory is occupied (see **Figure 7**). Local area 1, located within structural zone 7, is the most perspective. It is located within the junction of meridional, latitudinal and north-eastern faults. Local area 2 of this structural-tectonic zone occupies a similar structural position, but it is smaller than area 1. From the geological information on this territory, there is only structural map data (**Structural and tectonic map, 1996**) where no local structures have been established.

Within structural-tectonic zone 5, two small local areas 3 and 4 are established. Local area 3 is located with-

in the Bogoduhivska structure (**Structural and tectonic map, 1996**), there is no other information on this area. Local area 4 is located near the junction of the meridional fault 4.1 with the latitudinal fault 8.2.

Within structural-tectonic zone 4, there is one local prospective area 5, small in area, which is located within the junction of meridional, latitudinal, and north-eastern faults and coincides with the Danchakhiv structure on the map (**Structural and tectonic map, 1996**).

Within the established prospective areas, it is advisable to conduct detailed geophysical and atmogeochemical studies in order to assess their prospects in the future.

4. Conclusions

The faults highlighted on the lineament density maps coincide with the known faults that were established according to geological and geophysical data.

The analysis of the lineament density maps made it possible to identify more faults than were previously identified according to geological and geophysical data. At the same time, it is possible to distinguish faults of different scale levels.

During predictive studies, it was established that all maps of lineament density fields - both individual systems and the sum of lineaments and lineament intersection nodes - had an impact on the hydrocarbon reservoir placement (from 53% to 67.5% of objects of study are allocated by separate systems) and were therefore used for predictive assessment of the prospects areas. The use of the complex function of the likelihood ratio made it possible to identify more than 90% of the study objects.

A forecast map of hydrocarbon reservoirs was drawn up within the test site, where all known deposits and a part of oil and gas-bearing structures not verified by drilling data were reliably identified. The most productive deposits of the district were assessed with the highest prospective values, but productivity was not taken into account in the forecasting process. It is possible that the prospectivity values from the forecast data may indicate the productivity of the deposits, but this assumption needs further verification.

The 8 zones are distinguished within the test site based on the complex probability function map analysis, within which there are 5 perspective areas selected, and they make up 6% of the test site.

For a predictive assessment of 1, 2, 3 structural-tectonic zones, within which hydrocarbon reservoirs are known, more detailed predictive surveys should be conducted using the proposed methodology and remote sensing data of a high spatial resolution. At the same time, the study area should be limited only to the territory of the mobile structural zone.

The results of predictive studies of the Skvortsivsko-Yuliivsk polygon, based on the lineament analysis methods by remote sensing data and spatial probabilistic

forecasting methods proposed by the authors, testify to the feasibility of using these methods to solve similar problems in other oil and gas-bearing provinces.

5. References

- Ahmadi, H. and Pekkan, E. (2021): Fault-Based Geological Lineaments Extraction Using Remote Sensing and GIS— A Review. *Geosciences* 2021, 11, 183. <https://doi.org/10.3390/geosciences11050183>.
- Al Rawashdeh S., Bassam S. and Hamzah M. (2006): The use of Remote Sensing Technology in geological Investigation and mineral detection in El Azraq-Jordan. *European Journal of Geography, Systemes, Modelisation, Geostatistiques*, 2856, 203–219.
- Apostolov O. A. and Khodorovsky A. Ya. (2017): Methodology for forecasting hydrocarbon deposits based on lineament analysis data. Modern methods of remote search for minerals. In: V. I. Lyalko and M. O. Popov (eds). Kyiv, 59-64. 1 electron. wholesale disc (CD-ROM); ISBN 978-966-02-8295-7 (electronic edition). (in Ukrainian).
- Arlegui A. L. and Soriano M. A. (1998): Characterizing lineaments from satellite images and field studies in the Central Ebro basin (NE Spain). *International Journal of Remote Sensing*, 19(16), 3169-3185.
- Atlas of oil and gas deposits of Ukraine. In six volumes. (1998): N. III. Eastern oil and gas region. Collective author. Lviv: Publishing House "Center of Europe", 932-1416 (in Ukrainian).
- Atlas. Geology and minerals of Ukraine. arrange Institute of Geol. (2001): Sciences of the National Academy of Sciences of Ukraine, "Geos-XXI century" UICPT; L.S. Galletskyi (eds). 1: 5000000 Kyiv: State Enterprise "Taki spry", 168 p. (in Ukrainian).
- Baghriy I.D. (2013): Development of geological-structural-thermo-atmogeochemical forecasting of mineral exploration and assessment of the geocological state of the environment. K.: Logos, 511p. (in Ukrainian)
- Bagriy I.D., Gladun V.V. and other.(2007): Oil and gas prospecting objects of Ukraine. Forecasting of perspective oil and gas facilities in the Dnipro-Donetsk gas and oil-bearing region using a complex of non-traditional near-surface research methods. Kyiv, 535 p. (in Ukrainian)
- Bety, Azhar & Al-Jawadi, Azealdeen & Ismaeel, Omar. (2022): Lineament Analysis by Using Remote Sensing and GIS Technique of Sangaw Area, Kurdistan Region, NE Iraq. *Iraqi Geological Journal*, 55, 150-161. 10.46717/igj.55.2C.11ms-2022-08-24
- Burdick R. G. and Speirer R. A. (1980): Development of a method to detect geologic faults and other linear features from Landsat images. Report 8413. Bureau of Mines Report of Investigations US, 74 p.
- Casas A. M., Cortes A. L., Maestro A., Soriano M. A., Riaguas A., Bernal J. (2000): LINDENS: A program for lineament length and density analysis. *Computers & Geosciences*, 26 (9-10), 1011-1022.
- Chaabouni R., Bouaziz S., Peresson H., Wolfgang J. (2012): Lineament analysis of South Jenein Area (Southern Tuni-

- sia) using remote sensing data and geographic information system. The Egyptian Journal of Remote Sensing and Space Science, 15(2), 197-206. doi:10.1016/j.ejrs.2012.11.001.
- Chebanenko I.I. (1977): Theoretical aspects of the tectonic divisibility of the earth's crust. Kyiv, Naukova Dumka, 88p. (in Russian)
- Chekunov A.V. and Pashkevich I.K. (1989): Tectonic nature of magnetic heterogeneities in the lithosphere of Ukraine. Dokl. AN Ukrainian SSR. Serb. 5. (in Russian)
- Chirvinskaya M.V. and Sollogub V.B. (1980): Deep structure of the Dnieper-Donetsk aulacogen according to geophysical data. Kyiv, Nauk. Dumka, 180 p. (in Russian)
- Cortés A. L., Maestro A., Soriano M. A., Casas A. M. (1998): Lineaments and fracturing in the Neogene rocks of the Almazan Basin, northern Spain. Geological Magazine, 135(2), 255-268.
- De Oliveira Andrades Filho C., De Fa ´tima Rossetti D. (2011): Effectiveness of SRTM and ALOS-PALSAR data for identifying morphostructural lineaments in northeastern Brazil. International Journal of Remote Sensing, 33 (4), 1058–1077. <https://doi.org/10.1080/01431161.2010.549852>.
- Drury S. A. and Berhe S. M. (1993): Accretion tectonics in northern Eritrea revealed by remotely sensed imagery. Geological Magazine, 130, 177–190.
- Ehmann W. J. (1985): Lineaments and their association with metal deposits, Ruby Mountains, Montana. Department of the interior U.S. Geological Survey, R290 no.85-599 D, 15 p.
- Eleni Kokinou and Costas Panagiotakis (2020): Automatic Pattern Recognition of Tectonic Lineaments in Seafloor Morphology to Contribute in the Structural Analysis of Potentially Hydrocarbon-Rich Areas. Remote Sensing, 12, 1-18. [10.3390/rs12101538](https://doi.org/10.3390/rs12101538).
- Elmahdy S. I. and Mohamed M. M. (2016): Mapping of tectonelements and investigate their association with earthquakes in Egypt: a hybrid approach using remote sensing data. Geomatics Nat. Hazards Risk, 7, 600–619. <https://doi.org/10.1080/19475705.2014.996612>.
- Garetsky R.G., Glushko V.V., Krylov N.A. (1988): Tectonics of the oil and gas-bearing regions of the south-west of the USSR. Moscow, Nauka, 85 p. (in Russian)
- Ghislain Ngassam Mbianya, Timoleon Ngotue, Jonas Didero Takodjou Wambo, Sylvestre Ganno, Amin Beiranvand Pour, Patrick Ayonta Kenne, Donald Hermann Fossi, Isabelle D. Wolf (2021): Remote sensing satellite-based structural/alteration mapping for gold exploration in the Ketté goldfield, Eastern Cameroon, Journal of African Earth Sciences, 184, 104386, <https://doi.org/10.1016/j.jafrearsci.2021.104386>
- Halybyna I.V., Katterfeld G.N., Charushyn G.V. (1975): Types and systems of planetary lineaments. Journal of the Academy of Sciences of the USSR, ser. Geol., 11, 5-28. (in Russian)
- Havrysh V.K. (1969): Deep structures (faults) and methods of their study. Kyiv. Scientific opinion. 269 p. (in Russian)
- Havrysh V.K., Zabello G.D., Ryabchun L.Y. and others. (1989): Geology and petroleum gas production of the Dnieper-Donetsk Basin. Deep structure and geotectonic development. Opening ed. V.K. Havrysh; Academy of Sciences of the Ukrainian SSR. Institute of Geological Sciences. Kyiv. Scientific Opinion. 208 p. (in Russian)
- Henkel H. (1979): Dislocation sets in Northern Sweden. Geologiska Foreningens i Stockholm Forhandlingar, 100, 271–278.
- Henkel H. (1992): Geophysical aspects of meteorite impact craters in eroded shield environment—with emphasis on electric resistivity. Tectonophysics, 216, 63–89.
- Henkel H., Puura V., Flode ´n T., Kirs J., Konsa M., Preeden U., Lilljequist R., Fernlund J. (2005): Avike Bay — a 10 km diameter possible impact structure at the Bothnian Sea coast of central Sweden. In: Koeberl, C., Henkel, H. (Eds.). Impact Tectonics. Berlin, Heidelberg, New York: Springer, 323–340.
- Hudson J. A. and Priest S. D. (1979): Discontinuity and rock mass geometry. International Journal of Rock Mechanics and Mining Sciences and Geomechanics, 16, 339–362.
- Hudson J. A. and Priest S. D. (1983): Discontinuity frequency in rock masses. International Journal of Rock Mechanics and Mining Sciences and Geomechanics, 20, 73–89.
- Jinfei W. and Howarth P. J. (1990): Use of the Hough transform in automated lineament. IEEE Trans. Geosc. Remote Sens, 28 (4), 561–567.
- Jordan G., Meijninger B.M.L., Van Hinsbergen D.J.J., Meulenkamp J.E., Van Dijk P.M. (2005): Extraction of morphotectonic features from DEMs: Development and applications for study areas in Hungary and NW Greece. Inter. J. Appl. Earth Obser. Geoinform, 7, 163–182.
- Jordan G. and Schott B. (2005): Application of wavelet analysis to the study of spatial pattern of morphotectonic lineaments in digital terrain models: a case study. Remote Sens. Environ, 94, 31–38.
- Joshi A. K. (1989): Automatic detection of lineaments from landsat data. Geosci. Remote Sens, 1, 85–88.
- Juhari M. A. and Ibrahim A. (1997): Geological application of landsat tm imagery: mapping and analysis of lineament in NW Peninsula Malaysia, in: Proceedings of the 18th Asian Conference on Remote Sensing, 132–140.
- Jutz S. L. and Chorowicz J. (1993): Geological mapping and detection of oblique extensional structures in the Kenyan Rift Valley with a SPOT/LANDSAT-TM data merge. International Journal of Remote Sensing, 14, 1677–1688.
- Kageyama Y., Nishida M., Oi T. (2000): Analysis of the segments extracted by automated lineament detection, in: Geoscience and Remote Sensing Symposium, Proceedings, 1, 289–291.
- Khodorovsky A. Ya. and Apostolov A. A. (2012): Lineament analysis in the predictive assessment of the oil and gas potential of the territory. Satellite methods of searching for minerals. In: V. I. Lyalko and M.A. Popov (eds). Kyiv, Carbon-Ltd. 216-237. (in Russian)
- Khodorovsky A.Ya. and Apostolov A.A. (2014): Analysis of the dependence of the number of distinguished lineament systems on the width of the grouping interval. Dopovidi NAS of Ukraine. 9, 79-85. <https://doi.org/10.15407/dopovidi2014.09.079>. (in Russian)

- Khodorovsky A. Ya. and Apostolov A. A. (2013): Method for quantitative selection of lineament systems. *Dopovidi NAS of Ukraine*, 1, 111–117. (in Russian)
- Kim G., Lee J., Lee K. (2004): Construction of lineaments maps related to groundwater occurrence with arc view and avenue scripts. *Computers and Geosciences*, 30 (9/10), 1117–1126.
- Koike K. and Ichikwa, Y. (2006): Spatial correlation structures of fracture systems for deriving a scaling law and modeling fracture distributions. *Computers and Geosciences*, 32, 1079–1095.
- Koike K., Nagano S., Ohmi M. (1995): Lineament analysis of satellite images using a segment tracing algorithm (STA). *Computers and Geosciences*, 21, 1091–1104.
- Kropotkin P.N. (1985): Degassing of the Earth and the origin of hydrocarbons. *Bull. MOIP (department of geol.)*. 60(6), 3 – 18. (in Russian)
- Lattman L. H. and Parizek R. R. (1964): Relationship between fracture traces and the occurrence of ground water in carbonate rocks. *Journal of Hydrology*. 2, 73–91.
- Leary D. W., Friedman J. D., Pohn H.A. (1976): Lineament, linear, lineation: some proposed new standard for old term. *Geo. Soc. Amer. Bulletin*, 87, 1463–1469.
- Lim C. S., Ibrahim K., Tjia H. D. (2001): Radiometric and Geometric information content of TiungSat-1 MSEIS data, in: *TiungSAT-1: From Inception to Inauguration*, 169–184.
- Lyalko V. I., Khodorovsky A. J., Apostolov A. A., Vostokov A. (2010): B. Quantitative prognosis of oil and natural gas fields. *ISPRS TC VII Symposium – 100 Years ISPRS*. Vienna. Austria. *IAPRS, XXXVIII (7B)*, 622 – 627.
- Mabee S. B., Hardcastle K.C., Wise D.U. (1994): A method of collecting and analyzing lineaments for regional-scale fractured-bedrock aquifer studies. *Ground Water*, 32 (6), 884–894.
- Magesh N. S., Chandrasekar N., Soundranayagam J. P. (2012): Delineation of groundwater potential zones in Theni district, Tamil Nadu, using remote sensing, GIS and MIF techniques. *Geosci. Front*, 3, 189–196. <https://doi.org/10.1016/j.gsf.2011.10.007>.
- Maryam Errami, Ahmed Algouti, Abdellah Algouti et al (2022): Mapping and analysis of structural lineaments using SRTM radar data and Landsat 8-OLI images in Telouet-Tighza area, Marrakech High Atlas - Morocco., 25 February 2022, PREPRINT (Version 1) available at Research Square. <https://doi.org/10.21203/rs.3.rs-1153424/v1>
- Masoud A. and Koike K. (2011): Auto-detection and integration of tectonically significant lineaments from SRTM DEM and remotely-sensed geophysical data. *ISPRS J. Photogr. Remote Sens*, 66, 818–832.
- Mohamed, M.T.A., Al-Naimi, L.S., Mgbeojedo, T.I. et al. (2021): Geological mapping and mineral prospectivity using remote sensing and GIS in parts of Hamissana, Northeast Sudan. *J Petrol Explor Prod Technol*, 11, 1123–1138. <https://doi.org/10.1007/s13202-021-01115-3>
- Moody J. and Hill M. (1956): Wrench fault tectonics. *Bull. Geol. Soc. Amer*, 67(9), 56–64.
- Mostafa E.M. and Qari M.Y.H.T. (1995): An exact technique of counting lineaments. *Engineering Geology*, 39, 5–16.
- Mostafa M. E. and Bishta A. Z. (2005): Significance of lineament patterns in rock unit classification and designation: a pilot study on the Gharib-Dara area, northern Eastern Desert. *Egypt. Int. J. Remote Sens*, 26 (7), 1463–1475.
- Mukherjee, Bishal & Kn, Radhika & Kumar, Tejas K. (2020): Lineament analysis using geoinformatics and its multi-criteria applications: a case study Bengaluru. Report number: 129, Paper ID : SBR/0720-202, 15(7). doi: 10.13140/RG.2.2.13154.35527/1
- Nagorsky V.A. (1971): Spatial and probabilistic forecasting. V. kn.: *Fundamentals of scientific forecasting of deposits of ore and non-metallic minerals*. Leningrad, 168–170. (in Russian)
- Nash C. R., Rankin L. R., Leeming P. M., Harris L. B. (1996): Delineation of lithostructural domains in northern Orissa (India) from Landsat Thematic Mapper imagery. *Tectonophysics*, 260, 245–257.
- Nikulin S. L. (2013): Geoinformation technology for solving forecasting and search problems based on a complex of geological, geophysical and space data. The dissertation for the degree of Doctor of Geological Sciences in the specialty 04.00.05 - Geological informatics. (in Russian)
- Onibudo Oluwasegun Oluwaseun, Amartey Ernest Nii Laryea, Kadiri Similoluwa Abiodun, Onibudo Olabamidele, Ajayi Seun A., Abdulkadir Sakariyau Babatunde, & Ahiahonu Desmond Senanu Loveridge. (2022): Lineaments mapping and digital analysis using remote sensing and geographic information system (GIS) in Erusu-Akoko area of Akoko North-West, Southwest Nigeria. <https://doi.org/10.5281/zenodo.6970677>
- Oskooi B. (2004): A broad view on the interpretation of electromagnetic data (VLF, RMT, MT, CSTMT). Ph.D. Dissertation. Uppsala University. Sweden, 68 p.
- Patent 32050 Ukraine, IPC (2006): G01V 9/00, G01V 11/00. Method of predicting mineral deposits. Lyalko V.I., Nagorskyi V.O., Khodorovskyi A.Ya., Apostolov O.A., Vostokov A.B. No. 200803560; application 03.20.2008. publ. 04.25.2008, Bull. No. 8. (in Ukrainian)
- Pererva V. M. (1999): Geofluidodynamic basis of satellite technologies for the search of industrial hydrocarbon accumulations. *New methods in aerospace geoscience*. Kyiv, LLC Carbon-Ltd, 165–194. (in Ukrainian)
- Priest S. D. And Hudson J. A. (1976): Discontinuity spacing in rock. *International Journal of Rock Mechanics and Mining Sciences and Geomechanics*, 13, 135–148.
- Raghavan V., Masumot S., Koike K., Nagano S. (1995): Automatic lineament extraction from digital images using a segment tracing and ration transformation approach. *Computers and Geosciences*, 30, 555–591.
- Raj K. G. (1989): Origin and significance of hem avathi – Tirthahalli megalineament – A concept. *Geosci. Remote Sens*, 1, 112–115.
- Redouane, M., Mhamdi, H., Haissen, F., Raji, M. and Sadki, O. (2022) Lineaments Extraction and Analysis Using Landsat 8 (OLI/TIRS) in the Northeast of Morocco. *Open Journal of Geology*, 12, 333–357. [10.4236/ojg.2022.125018](https://doi.org/10.4236/ojg.2022.125018)
- Saadi N. M., Abdel Zaher M., El-Baz F., Watanabe K. (2011): Integrated remote sensing data utilization for investigating structural and tectonic history of the Ghadames Basin, Libya. *Inter. J. Appl. Earth Obser. Geoinfor*, 13, 778–791.

- Salehi R., Saadi N. M., Khalil A., Watanabe K. (2015): Integrating remote sensing and magnetic data for structural geology investigation in pegmatite areas in eastern Afghanistan. *Journal of Applied Remote Sensing*, 9, 096097-1-096097-14. <https://doi.org/10.1117/1.jrs.9.096097>.
- Shults S.S. (1973): Planetary fracturing /basic provisions/. In: *Planetary fracturing*. Leningrad. Publishing house of the Leningrad University, 5-36. (in Russian)
- Structural and tectonic map of the DDZ (1996), scale 1:200,000, E.S. Dvoryanin (eds) (in Ukrainian)
- Sukumar M. and Nelson K. (2017): Performance evaluation of lineament extraction methods in ASTER satellite images. *International Journal of Oceans and Oceanography*, 11 (2), 249-263.
- Tovstyuk Z. M., Yefimenko T. A., Titarenko O. V., Svideniuk M. O. (2017): Remote Sensing Neotectonic Research on Oil and Gas Perspective Structures on the Example of the Dnieper-Donets Basin. *Journal of Georgian Geophysical Society*, 19(20), 75-83.
- Tyapkin K.F. (1998): *Physics of the Earth*. Kyiv, Vyscha shkola, 312p. (in Russian)
- Yevdoshchuk M.I., Chebanenko I.I. and others. (2001): Theoretical foundations of non-traditional geological methods of hydrocarbon search Kyiv, 287 p. (in Ukrainian)
- Zhantayev Z., Bibossinov A., Fremd A., Talgarbayeva D., Kikkarina A. (2017): Automated lineament analysis to assess the geodynamic activity areas. *Procedia Computer Science*, 121, 699-706.

SAŽETAK

Predviđanje potencijala naftnih i plinskih teritorija na temelju podataka daljinskih istraživanja, slučaj skvorcivsko-julievskoga ispitnog područja u Dnjiparsko-doneckoj depresiji u Ukrajini

Razvijene metodološke tehnike korištene su za procjenu propusnosti pukotina stijena i predviđanje ležišta ugljikovodika na primjeru skvorcivsko-julievskoga ispitnog područja Dnjiparsko-donecke depresije u Ukrajini. Propusnost stijena procijenjena je na temelju interpretacije strukturnih rezultata polja lineamenata pomoću podataka daljinskoga istraživanja. Odabrane su granice osam sustava lineamenata i njihove modalne vrijednosti te su sastavljene karte gustoće lineamenata. Rasjedi identificirani na kartama gustoće lineamenata odgovaraju rasjedima utvrđenim na temelju geoloških i geofizičkih podataka. Sastavljene su karte sumarne gustoće lineamenata i čvorova njihovih presjeka koje odražavaju propusnost pukotina stijena. Korištenjem tehnika prostorne probabilističke prognoze utvrđeno je da su sve karte polja gustoće lineamenta imale utjecaj na položaj ležišta ugljikovodika (od 53 % do 67,5 % objekata istraživanja raspoređeno je zasebnim sustavima) i korištene su za procjenu teritorija potencijala za istraživanje nafte i plina. Korištenje složene funkcije omjera vjerojatnosti omogućilo je identificiranje više od 90 % predmeta istraživanja. Karte predviđanja potencijala područja istraživanja u vezi s ležištima ugljikovodika sastavljaju se korištenjem kliznoga prozora veličine: 4,5 x 1,5 km i 14 x 4 km, što omogućuje predviđanje objekata istraživanja na različitim dubinama. Na temelju analize složene funkcije vjerojatnosti odabrano je osam zona. Odabrano je pet perspektivnih područja koja čine 6 % ispitnoga poligona.

Ključne riječi:

lineamenti, daljinsko mjerenje, predviđanje potencijala nafte i plina, perspektivna područja, Ukrajina

Author's contribution

Artur Khodorovskiy (PhD, Senior Researcher) participated in all work stages and provided the structure of the work, criteria definition and interpretations of the results. Alexander Apostolov (PhD, Scientific Researcher) provided software implementation of processing methods and received analysis data. Lesya Yelistratova (PhD, Senior Researcher) carried out data collection of satellite images and searched for geological information. Inna Romanciuc (PhD, Researcher) performed manuscript editing and graphical support.